Sensors and Actuators B 223 (2016) 893–903

Contents lists available at ScienceDirect

Sensors and Actuators B: Chemical

journal homepage: www.elsevier.com/locate/snb

Silver-doped zinc oxide single nanowire multifunctional nanosensor with a significant enhancement in response

Oleg Lupan[a,b,c,d,*], Vasilii Cretu[b], Vasile Postica[b], Mahdi Ahmadi[d], Beatriz Roldan Cuenya[d,e], Lee Chow[d], Ion Tiginyanu[b], Bruno Viana[c], Thierry Pauporté[c], Rainer Adelung[a,*]

[a] Functional Nanomaterials, Institute for Materials Science, Christian Albrechts University of Kiel, 24143 Kiel, Germany
[b] Department of Microelectronics and Biomedical Engineering, Technical University of Moldova, 168 Stefan cel Mare Blvd., MD-2004 Chisinau, Republic of Moldova
[c] PSL Research University, Chimie ParisTech-CNRS, Institut de Recherche de Chimie Paris, UMR8247, 11 rue P. et M. Curie, 75005 Paris, France
[d] Department of Physics, University of Central Florida, Orlando, FL 32816-2385, USA
[e] Department of Physics, Ruhr-University Bochum, 44801 Bochum, Germany

ARTICLE INFO

Article history:
Received 4 August 2015
Received in revised form
29 September 2015
Accepted 1 October 2015
Available online 9 October 2015

Keywords:
Nanocrystalline materials
ZnO:Ag
Nanowire
Nanosensor
Nano-photodetector

ABSTRACT

Enhanced performances were obtained for nanosensors based on a single nanowire of silver-doped zinc oxide (ZnO:Ag). Arrays of crystalline ZnO:Ag nanowires were synthesized by electrodeposition on F-doped tin oxide coated substrates and studied by SEM, EDX, TEM, HRTEM, SIMS, XPS, PL and micro-Raman spectroscopy. Integration of a single nanowire or a single microwire on the chip was performed by employing metal maskless nanodeposition in the dual beam focused electron/ion beam instrument. The ultraviolet (UV) response and hydrogen (H_2) gas response were studied for nanodevices and microdevices based on a single ZnO:Ag nanowire. We found that ZnO:Ag nanowire based nanosensor possesses a much faster response/recovery time and a higher response to UV radiation and hydrogen gas (~50%) than those reported in literature. An increase in current value of about two orders in magnitude I_{UVON}/I_{UVOFF} was observed under exposure to UV light. Faster response/recovery times of about 0.98 s/0.87 s were observed. The ZnO:Ag nanowires and microwires can serve as nano-building materials for ultrasensitive and ultra-fast sensors with reduced power consumption. The mechanisms for such improved responses to UV and H_2 were discussed. The developed nanomaterial is of great scientific interest for further studies as promising candidates for fabricating multifunctional nano-sensors, LEDs and photodetectors by bottom-up and hybrid nanotechnologies.

1. Introduction

Development of multifunctional nanosensors based on new advanced functional nano-materials is in the focus of the research community nowadays, since it is the largest and fastest evolving market segment, with revenues expected to surpass several trillion Euros soon. Scientific research on nano-materials contributes to miniaturization and improvements in the size, detection range, reliability, selectivity and sensitivity of existing solid-state sensors and light/image detectors, which are the key components of many electronic and optoelectronic circuits. Nanodevices which can perform multiple tasks are of high demand for intelligent portable device with small sizes (e.g. a cellphone, smartphone, sensors) and other applications (ranging from high-capacity information storage to biochemical sensing, chemical and biological analysis, and astronomy) due to very low power consumption. In this context, rapid detection of ultraviolet (UV) radiation, such as emission from combustion flames, is an important issue for industrial safety, especially when highly flammable gasses are involved (for example H_2) [1–5]. Of course, leakage of flammable gases should be detected first and it is desirable to be done by the same device. Development of such multifunctional detectors/sensors is in high demand to protect human health due to several critical factors, namely UV level is increasing due to ozone hole which latter may cause damage/cancer to the human skin, as well as highly flammable H_2 became a clean source of energy and starts to be used widely

* Corresponding authors at: Institute for Materials Science, University of Kiel, Germany.
E-mail addresses: ollu@tf.uni-kiel.de (O. Lupan), Beatriz.Roldan@rub.de (B.R. Cuenya), Lee.Chow@ucf.edu (L. Chow), bruno.viana@chimie-paristech.fr (B. Viana), thierry-pauporte@chimie-paristech.fr (T. Pauporté), ra@tf.uni-kiel.de (R. Adelung).

http://dx.doi.org/10.1016/j.snb.2015.10.002
0925-4005/

[1–7]. Our main goal is to investigate and develop multifunctional nanosensors, which can perform multiple tasks, such as UV detection, H_2 sensing and others by using the same device-construction. The main issue is the fabrication of higher sensitivity/selectivity, and faster response, one-dimensional gas sensors. Thus, semiconducting oxide nanowires (NWs) are perfect candidates, since they have been investigated extensively as core materials in various nanoscale sensing structures. ZnO was selected as a main candidate, as nano-building block since it is an important *n*-type semiconductor with a large band gap E_g = 3.37 eV at 300 K and it is a simple technology for further bottom-up approach [1–4]. ZnO nanostructures such as nanoparticles, nanowires, nanorods, and thin films are well known for their potential applications in nanoscale sensing and optoelectronic components, including biochemical and gas sensors [4], UV photo detectors [1–3,5], dye-based solar cells [6], and others [1–6]. In particular, nanodevices consisting of a single zinc oxide (ZnO) NW and NR have been investigated in selective and sensitive nanoscale gas sensors and light detectors for a wide range of potential applications [1–7]. It has been found for ZnO NWs that the presence of doping with metals or of charge trapping states at the surface drastically affects the gas response [5,7] and the photoconductivity because of the high surface-to-volume ratio in NWs [1–6]. In the ZnO wide-bandgap material, the high internal gain mediated by the surface state and doping is responsible for the enhanced photoresponse. Similar effect, on the other hand, has not been reported yet for silver-doped ZnO photodetectors. Previous reports clearly indicate the diminution of the concentration of donor defects due to doping by Ag for the compensation of the *n*-type conductivity [8], which could be of great practical interest in controlling device performance. Thus, attractive building blocks for multifunctional nano-materials, especially, quasi-one-dimensional (Q1-D) ZnO:Ag structures may become the most promising candidates for sensing applications in the near future due to their special geometry, acceptor type and new chemical–physical properties [2–4,8]. This is important since for Q1-D ZnO NWs the electrical resistance changes due to the interaction of the targeted gas molecules (chemi- or physi-sorption) with the surface of the ZnO nanowire/nanorod. Consequently, ZnO:Ag-sensors are expected to show higher and faster changes in the conductivity under exposure to UV radiation due to reduced level of electrons, smaller dimensions of conduction channel, thus reduced number of chemisorbed species on its surface, which makes it highly demanded for sensing applications for nanoscaled electronic and opto-electronic devices.

In this context, we investigate effects of Ag-doping of ZnO nanowire arrays on their properties [9,10]. The doping of zinc oxide by different metals was successful for controlling the properties [11]. However, for low-dimensional ZnO:Ag structures such as single nanowire devices, there exists a lack of scientific information. It is known, that the group Ib metals are fast-diffusers in compound semiconductors [9,10,12]. Ag, as an amphoteric dopant in ZnO, can be at the interstitial sites or at the substitutional Zn^{2+} sites [13] as reported previously [9,12].

The diffusion of Ag into ZnO can induce the formation of complex centers (Ag_{Zn}, Ag_i) [8–10,12]. It is possible that Ag atoms can replace either substitutional or interstitial Zn atoms in the ZnO lattice and create structural deformations [9,10,12]. Ag doping significantly affects the electrical, chemical, structural and optical properties of ZnO, and the study of the electronic state of dopant in ZnO is a great subject of research interest too [8–10,12]. In this work, we present a comparison of pure ZnO and ZnO:Ag single nanowire-based UV photodetectors and hydrogen nanosensors in the same device-structure with improved response performances at room temperature. Results were also compared with single nanobelt SnO_2 based nanosensors. We found that multifunctional nanosensors based on a single nanowire of ZnO:Ag have a faster response/recovery time to UV radiation than pure ZnO NW/NR, which was reported previously [1,4,6].

2. Experimental details

ZnO:Ag nanowire arrays were grown on F-doped tin oxide (FTO) film supported on a glass substrate with a resistance of 10 Ω/□ using an electrochemical deposition (ECD) process [5–7,10]. The parameters of the electrodeposition are: an electrical potential of −0.58 V versus SCE, a total charge per unit area of $-64\,C\,cm^{-2}$, a deposition temperature of 91 °C [5–7,10], and a total growth time of 200 min. After ECD, the samples were subsequently rinsed with DI water and dried in air to remove un-reacted products from the surface. Subsequently, the samples were subjected to thermal annealing in air at 250 °C for 12 h to relax the ZnO lattice. Scanning electron microscopy (SEM) images were acquired with a scanning electron microscope Ultra 55 Zeiss FEG (7 kV). The synthesized structures were characterized with a high-resolution X-ray diffractometer (Siemens D5000) operated at 40 kV and 45 mA using the $CuK\alpha_1$ radiation (λ = 1.5406 Å). Secondary ion mass spectrometry (SIMS) was used for the analysis of the Ag contents because of its excellent sensitivity and depth resolution [5–7,10]. SIMS measurements were carried out with a Physical Electronics ADEPT 1010 quadrupole analyzer with a 3 keV Cs^+ primary beam at 60° from the normal. The typical primary beam current was 25 nA. The primary beam was rastered over a 300 μm by 300 μm area, with the detection of negative secondary ions from an area of 100 μm by 100 μm at the center of the rastered area. Details of the experimental procedures can be found in previous reports [5–7,9,10,12]. The ex situ prepared samples were transferred into an ultrahigh vacuum system (UHV) system for chemical analysis via monochromatic X-ray photoelectron spectroscopy (XPS). Sample charging was corrected using adventitious carbon as binding energy (BE) reference (C-1s peak at 285 eV). For the quantitative analysis, the raw XPS spectra were fitted with Gaussian–Lorentzian functions. Due to spin–orbit coupling, the intensity ratios between the $2p_{3/2}$ and $2p_{1/2}$ Zn and Ag doublets were held constant at a value of 2. The concentration of the Ag dopant was estimated from the Cu-2p/Zn-2p ratio after proper normalization using the corresponding atomic sensitivity factors (ASF) [5,9,12].

A WITec Raman equipment was used for Raman scattering characterization of the nanowires. Excitation of samples was provided by a 532 nm line from a frequency doubled Nd:YAG laser at an output power of 10 mW [5–7,10]. The photoluminescence (PL) was studied at room temperature following a procedure described in a previous report [10,12].

The nanosensors were built by connecting a single ZnO:Ag nanowire to the chip substrate (SiO_2/Si with Au contacts as contact electrodes) using metal maskless nanodeposition in the dual beam focused electron/ion beam (FIB/SEM) instrument Dualbeam Helios Nanolab (FEI) (5 kV, 0.17 nA). The single-nanowire contacts were imaged using FESEM. Consistent experimental data from several single nanowire devices were obtained. Additional details on the connection of very thin ZnO NW (about 100 nm in diameter) using FIB/SEM are given in our recent works [5,6]. It should be pointed out a major difference in comparison to previous reports is that during fabrication a single ZnO:Ag NW device structure, a single NW was exposed to the electron beam for less than 1 min, only the edges of NW where exposed to the beam about 2–3 min. The enhanced radiation hardness of ZnO NWs as compared to bulk ZnO layers was also reported in previous works [5,6]. The H_2 sensing characteristics of a nanosensor structure were studied as described before [5]. The concentration of H_2 gas was measured using a precalibrated mass flow controller. A computer with suitable LabView interface handled all controls and acquisition of data. Hydrogen

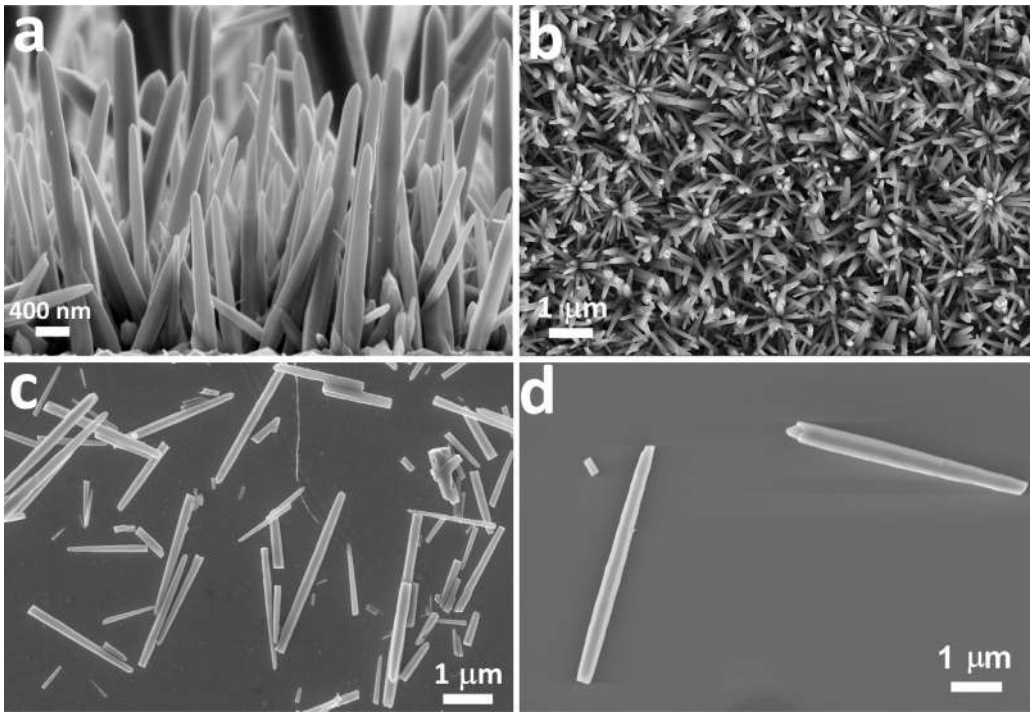

Fig. 1. SEM micrographs of ZnO:Ag (1 μM $AgNO_3$ in the electrolyte) nanowire arrays electrodeposited on an FTO substrate: (a) cross-sectional view; (b) top-view of sample shown in (a); (c) then transferred by direct touching to an intermediate SiO_2/Si substrate for further dispersion to a lower density of distribution on the surface; (d) afterwards transferred by direct touching the next intermediate SiO_2/Si substrate for its further integration in nanosensor structures.

and air were introduced to a gas mixer via a two-way valve using separate mass flow controllers. The mixed gas was injected to a test chamber with a sensor holder, in which the nanosensor was placed [14–16]. By monitoring the output voltage across the NW-based sensor, the conductance was measured in air, under UV and in the test gas, respectively. The gas sensing and photodetection performances of structures toward UV radiation pulses at 365 nm were investigated as described below and in our previous works [5–7,10]. The detection of UV light is performed through using H135 UV source, Labino Compact UV lamps (Labino AB, Sweden) at intensity of 10–20 mW cm^{-2}, measured using a photodiode [17]. All measurements were performed in a quasi-steady state.

3. Experimental results

3.1. Morphological, TEM, chemical, electronic and micro-Raman investigations

Fig. 1 illustrates a typical morphology of ZnO:Ag nanowire arrays on FTO substrate grown by the ECD process at 91 °C. These ZnO:Ag NWs are fairly uniformly distributed on the substrate (Fig. 1(a and b)). Cross-sectional view (Fig. 1(a)) clearly shows that ZnO:Ag NWs are oriented upward with respect to the FTO film underlying glass substrate. The image shows that each ZnO NW has a quasi-1-D (Q1-D) shape with a length of about 4 μm and diameters of 100–400 nm. Its length and thickness depends on the duration of ECD process

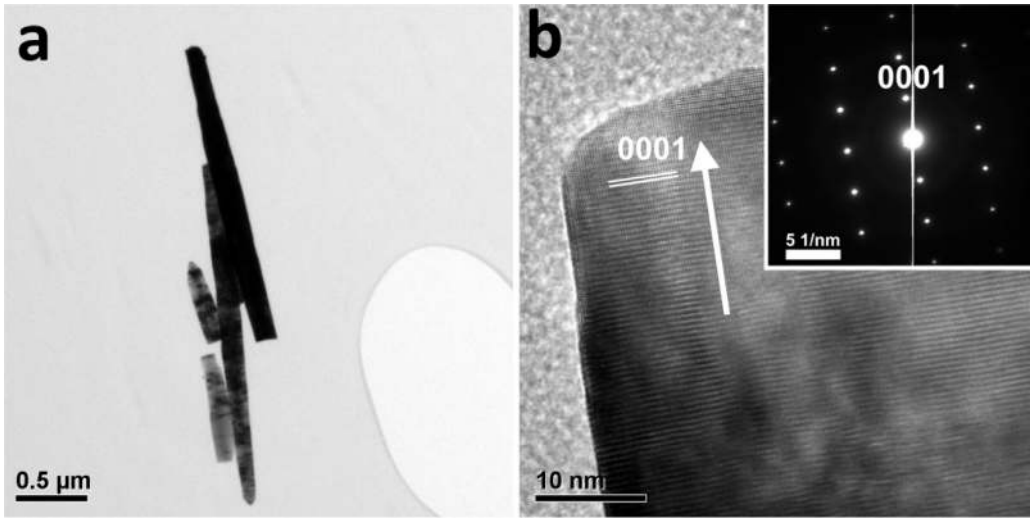

Fig. 2. (a) TEM image of the ZnO:Ag (1.0 μM $AgNO_3$ in the electrolyte) nanowires revealing the surface morphology and shape. (b) HRTEM image of the ZnO:Ag nanowire shown in (a). The insert shows an SAED electron diffraction pattern of the same sample, which is representative for different investigated regions.

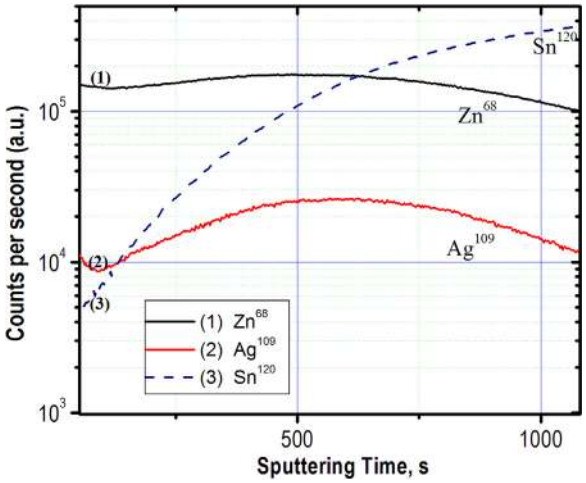

Fig. 3. SIMS measurements of ZnO:Ag nanowires (1.0 μM $AgNO_3$ in the electrolyte) grown on F-doped tin oxide substrate. The dashed curve (Sn) corresponds to the substrate.

[10]. Fig. 1(b) shows top-view SEM image of a ZnO:Ag nanowire arrays on FTO substrate. Fig. 1(c) presents numerous NWs transferred from the initial substrate by touching to an intermediate SiO_2/Si substrate for further dispersion to a lower density of NWs on the surface. Fig. 1(d) shows a single NW transferred by touching an intermediate SiO_2/Si substrate for further integration in nanosensor structures. Detailed morphological studies of all concentrations of ZnO:Ag NW arrays on FTO and GaN can be found in previous work [10].

Fig. 2(a) shows the TEM bright field image of an individual ZnO:Ag nanowire on carbon holey TEM grid. It can be seen that the NW thickness on the bottom is about 200–300 nm, and gradually narrowing near the top. The surface appears to be very smooth while the top surfaces are faceted, showing a hexagonal pattern. These features indicate that each NW is probably a single crystal along the ⟨0 0 0 1⟩ *c*-axis growth direction. These characteristics are further confirmed by HRTEM analysis. Fig. 2(b) presents a HRTEM image together with an inset showing the corresponding selected area electron diffraction (SAED) pattern. It is indicating that each ZnO NWs is a single crystal with wurtzite structure in all studied regions. The corresponding zone axis was determined to be [0 0 0 1]. The growth mechanism for ZnO:Ag NWs is believed to be similar to the one described for pure zinc oxide nanowires synthesized by ECD process [6,10].

The composition of the ZnO:Ag NWs product was analyzed by EDX as discussed above and reported previously [10]. For example, initial [$AgNO_3$] in the aqueous electrolyte was 1.0 μM. The [Ag(I)]/[Zn(II)] ratio in the starting aqueous electrolyte was 0.5%. Atomic Ag content determined by EDX was found to be 1.8%, defined as the [Ag]/[Ag+Zn] ratio. Typical XRD pattern was shown in our previous report [10] indicating that the product has a wurtzite structure with cell constants of $a = 3.25$ Å and $c = 5.21$ Å (JCPDS card 036-1451). The chemical composition of the nanowires was investigated by SIMS. Fig. 3 shows Zn, Ag and Sn signals from the ZnO:Ag (1.0 μM) NW on FTO versus the sputtering time. The Ag count rate closely follows the Zn count rate over most of the sample depth. This is an indication that Ag has been evenly incorporated into the ZnO nanowire structure. As expected, no correlation between the Ag and Sn (from the FTO substrate) count rates was observed, and a gradual increase in the Sn signal until saturation is reached and observed as a function of the sputtering time. The experiment suggests that the Ag content is about 1.8%, in this sample [10]. Similar results were obtained for other samples and not shown here to avoid repetition.

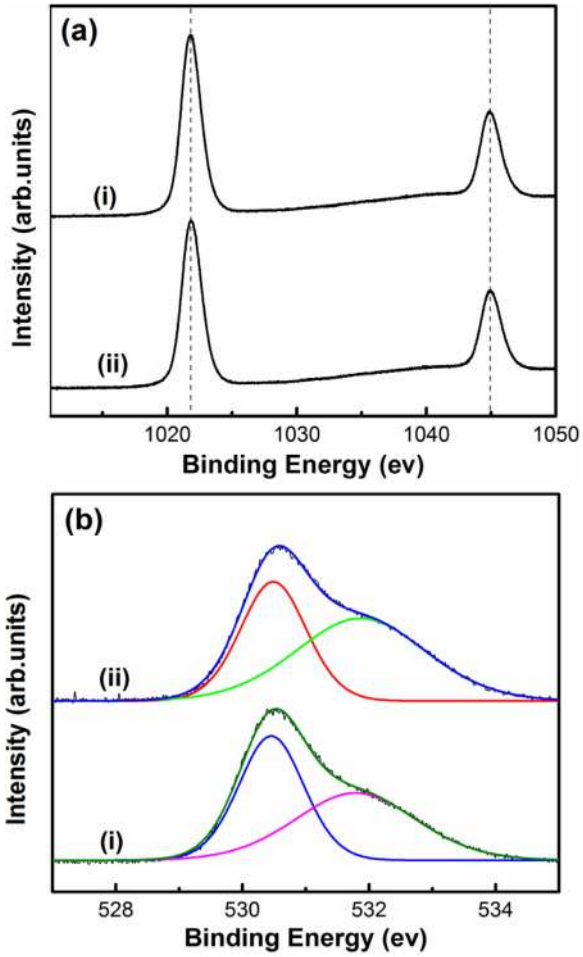

Fig. 4. XPS spectra (Al Kα = 1486.6 eV) corresponding to the: (a) Zn-2p; and (b) O-1s core level regions of (i) 0.5 μM Ag-doped and (ii) 2.0 μM Ag-doped ZnO nanowire arrays.

XPS was used to characterize the composition of ZnO:Ag (0.5 μM) and ZnO:Ag (2.0 μM) nanowire samples. Positive binding energy (BE) shifts were observed in the XPS spectra due to charging effects. Therefore, the BE scale was calibrated using the adventitious carbon peak (C-1s) at 285 eV as reference. In our samples, residual amounts of adventitious carbon and carbonyl compounds are unavoidable due to their exposure to air prior to the XPS analysis [15].

Fig. 4(a) shows XPS spectra of the Zn-2p core level region of ZnO:Ag nanowires. The spectra could be fitted with a doublet at 1021.9 and 1045 eV (vertical reference line) corresponding to the Zn-$2p_{3/2}$ and $2p_{1/2}$ core levels. The asymmetric feature observed in the O-1s region, Fig. 4(b), was fitted by two subspectral components corresponding to stoichiometric ZnO (530.5 eV) and defective ZnO_x (531.8 eV) [18].

The Ag-3d XPS BE region of the ZnO:Ag samples is shown in Fig. 5. The two asymmetric peaks could be fitted with two doublets tentatively assigned to the $Ag_{3d5/2}$ and $Ag_{3d3/2}$ core levels of two different species: (i) cationic Ag in ZnO ($Ag_{3d5/2}$ = 367.6 eV, 88% of the total Ag XPS signal of sample 2.0 μM Ag-doped ZnO, 86% of sample 0.5 μM Ag-doped ZnO) and (ii) metallic Ag ($Ag_{3d5/2}$ = 368.7 eV, 12%, 14% for the 2 μM and 0.5 μM Ag-doped ZnO samples, respectively) [19–22]. There is a remarkable shift between Ag in ZnO and the standards measurement for bulk Ag (368.7 eV), with a BE slightly lower than Ag^+ (367.8 eV), indicating the strong interaction of Ag cations with ZnO.

Micro-Raman measurements are an effective approach for fast and nondestructive study of dopant incorporation [9,12].

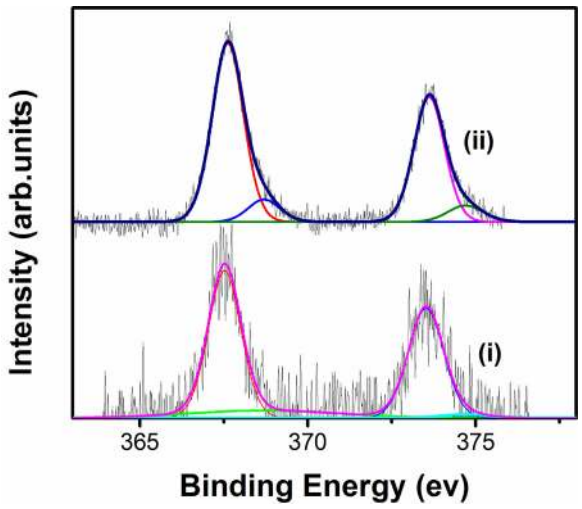

Fig. 5. XPS spectra (Al Kα = 1486.6 eV) corresponding to the Ag-3d core level region of (i) ZnO:Ag (0.5 μM), (ii) ZnO:Ag (2.0 μM) nanowire arrays.

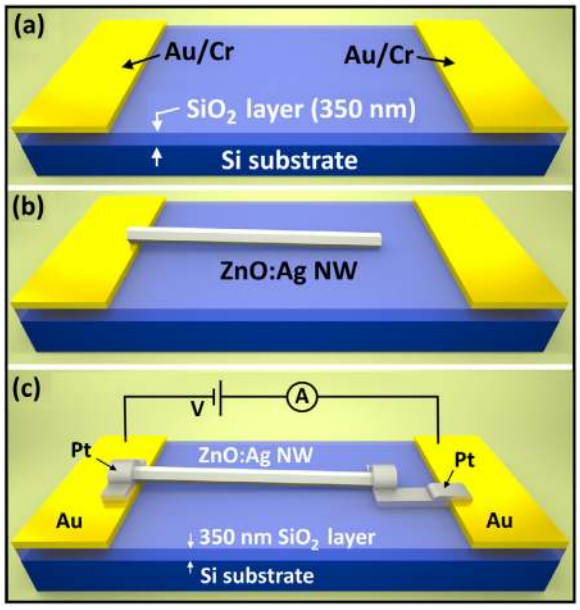

Fig. 7. Illustration of the process for fabrication of two-terminal nanodevice using Au/Cr electrodes prepatterned SiO_2/Si substrate (a). The thickness of a SiO_2 layer was 350 nm. In first step, the ZnO:Ag NW was transfered to SiO_2-coated Si prepatterned substrate (b). After this, the two Pt complex rigid contacts were made at both ends of the NW using dual beam FIB/SEM system to form interconnections with Au/Cr electrodes (c). Method of connection configuration for electrical, UV and hydrogen gas measurements is also presented (c).

Room-temperature, normalized micro-Raman spectra of the pure and ZnO:Ag nanowire arrays are shown in Fig. 6(a). ZnO with a Wurtzite structure belongs to the C_{6v}^4 ($P6_3mc$) space group and there are 12 degrees of freedom since there are 4 atoms per primitive cell. According to the group theory analysis, only A_1, E_1, and E_2 vibrational modes are Raman active phonons [23]. Dominant peaks at 100 cm^{-1} and 438 cm^{-1}, which are commonly detected in the wurtzite structure ZnO [23], are attributed to the low- and high-E_2 mode of non-polar optical phonons, respectively, and indicate on high crystalline quality of the ZnO nanowires. The Raman peaks at 382 cm^{-1} and 410 cm^{-1} can be assigned to the $A_1(TO)$ mode and $E_1(TO)$ mode of ZnO, respectively. Two smaller peaks at 334 cm^{-1} and 381 cm^{-1} are observed in Fig. 6(a) and correspond to E_{2H}–E_{2L} (multi phonon) and A_{1T} modes. The peaks corresponding to the E_2(low) and E_2(high) phonon mode reflect the perfection of the ZnO crystal [23–25]. By increasing of the Ag content in the ZnO nanowires, the intensity of the E_2(high) phonon mode is slightly decreased, indicating on evenly Ag^+ incorporation [25,26]. The induced crystal damage of ZnO may be caused by host lattice defects such as vacancies and interstitials and is considered as an indication of dopant incorporation [9,12]. At high concentration of Ag content some major changes in the micro-Raman spectra are observed. The broad band at 144 cm^{-1} can be attributed to lattice vibration. A downshift of E_2(high) phonon mode to 435.7 cm^{-1} indicates a redistribution of electron density due to the generation of point defects after Ag doping, which have a strong influence on the oxygen sublattice [9,12,27].

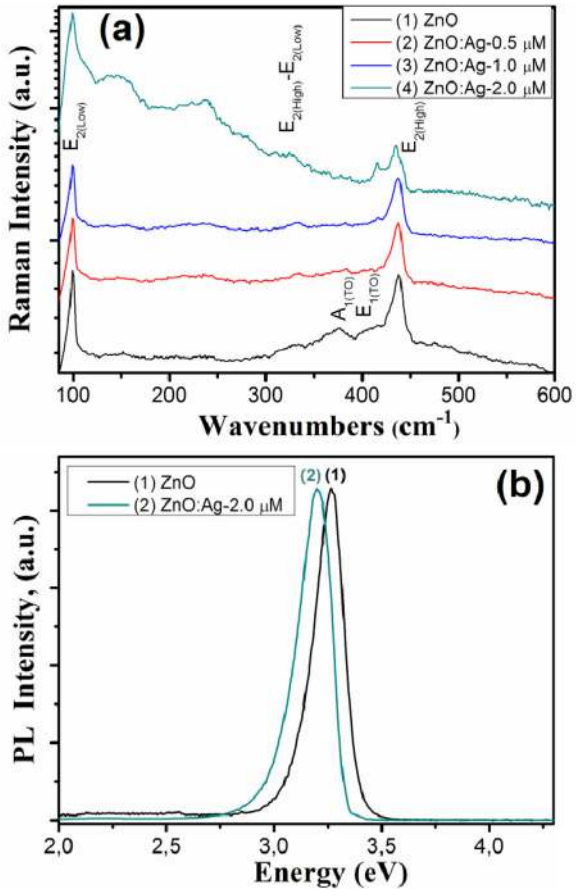

Fig. 6. Micro-Raman spectra (a) and photoluminescence spectra (b) of pure ZnO NWs and ZnO:Ag (0.5, 1.0 and 2.0 μM $AgNO_3$ in the electrolyte and indicated on each graph) nanowire arrays.

The photoluminescence (PL) spectra have been measured at room temperature and are presented in the normalized form in Fig. 6(b). The nanowire arrays are characterized by a strong near-band edge emission in the near-UV wavelength region. No visible emission due to defects is observed either for the pure ZnO, or of the ZnO:Ag nanowires at 2.0 μM, respectively. The NW arrays are of high structural quality. The PL emission is slightly shifted toward a longer wavelength by several nm with the Ag-doping in samples, which is consistent with previous observations [3,28,29].

3.2. *Nanosensors fabrication and their multifunctional performances*

For a single ZnO:Ag NW based nanosensor fabrication we used specially designed Au/Cr electrodes patterned SiO_2/Si substrate (schematically shown in Fig. 7(a)) to increase probability of

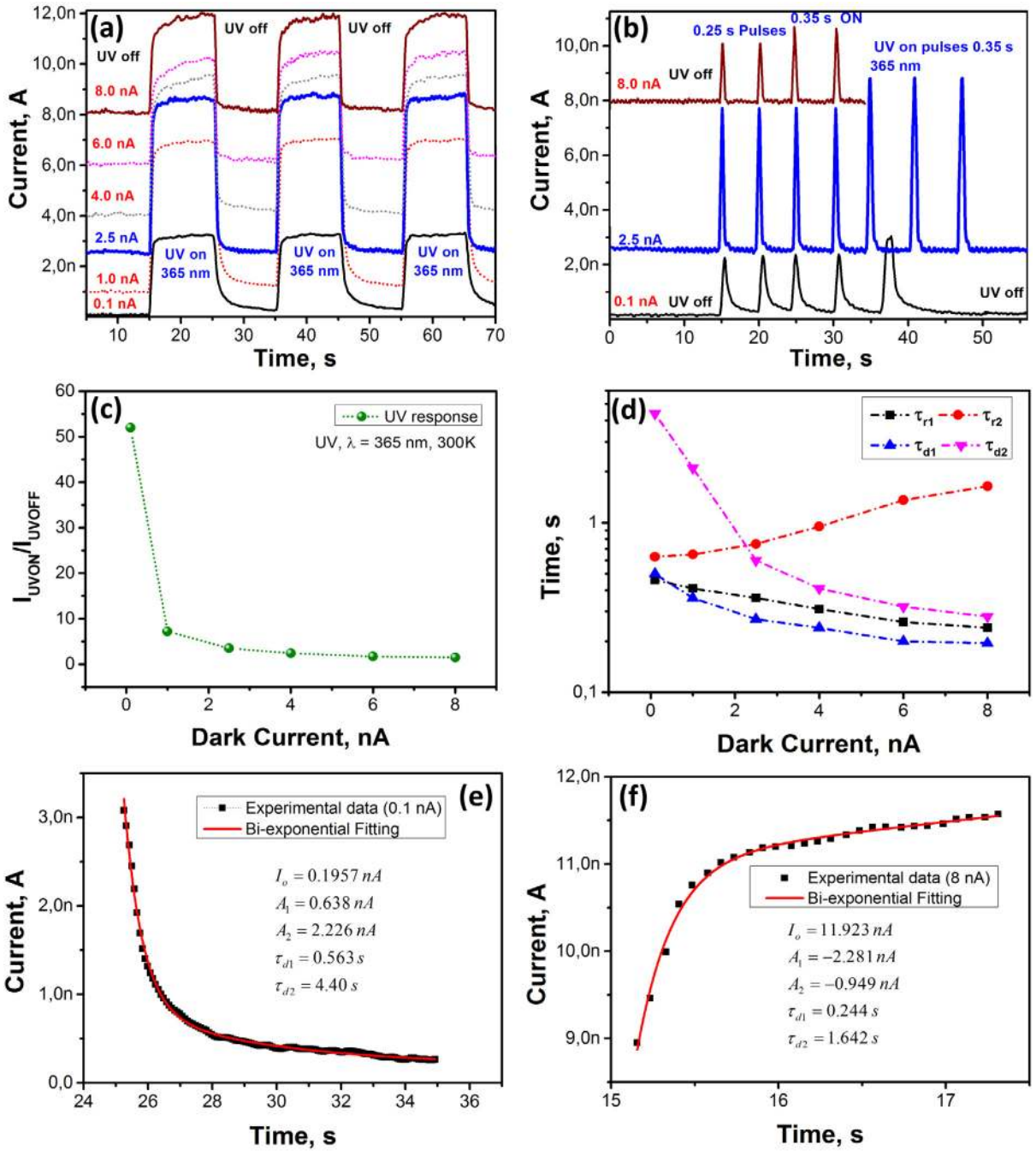

Fig. 8. (a) Reversible switching of the electrical current from the device structure made on a single ZnO:Ag nanowire under 60 s periodic illumination of UV light measured in air at different values of the dark current (0.1, 1.0, 2.5, 4.0, 6.0 and 8.0 nA). (b) Reversible switching of the electrical current with 0.25 s and 0.35 s periodic illumination of UV light for device at dark current value of 0.1, 2.5 and 8.0 nA. (c) Current ratio I_{UVON}/I_{UVOFF} of the nanosensor versus applied bias voltage at room temperature. (d) Time constants (τ_{r1}, τ_{r2}, τ_{d1} and τ_{d2}) for nanodevice versus applied bias voltage at room temperature. (e) Bi-exponential fitting of photoresponse decay curve for nanosensor at dark current of 0.1 nA. (f) Bi-exponential fitting of photoresponse rise curve for nanosensor at dark current of 8.0 nA.

nanowires being dispersed between the electrodes. After transfer of ZnO:Ag NW to a SiO_2-coated (350 nm) Si substrate (schematically shown in Fig. 7(b)), the both ends of NW were contacted in a dual beam FIB/SEM system with Pt complex for formation of two terminal nanodevice (schematically shown in Fig. 7(c)), as was reported in our previous works [5,15,30]. The method of connection configuration for electrical, UV and hydrogen gas measurements is presented in Fig. 7(c).

The hydrogen gas sensing properties were also investigated. Fig. S1 shows reversible switching of electrical current from nanodevice based on a single ZnO:Ag NW at exposure to two pulses of 100 ppm H_2 gas. The gas response is presented by ratio $S_{H_2} = \Delta I/I_{gas}$, where $\Delta I = I_{gas} - I_{air}$, I_{gas} and I_{air} are the current values of the nanosensor under exposure to hydrogen gas and ambient air, respectively. Fabricated nanodevice (samples of ZnO:Ag nanowires with 1.0 μM $AgNO_3$ in the electrolyte) demonstrated a gas response of ~50% at room temperature (RT, 300 K) with good recovery to the initial baseline, taking ~22 s for 90% of full response and ~12 s for 90% of complete recovery.

Next, the UV response of the fabricated nanodevices will be investigated. Fig. 8(a) shows reversible switching of electrical current with 60 s periodic illumination of UV light (λ = 365 nm)

Table 1
Comparison of the hydrogen gas sensors performances based on a single Q1D structure.

Material, morphology	Diameter (nm)	H_2 conc. (ppm)	Gas response (%)	Operating temperature (°C)	Response/rise time (s)	Recovery/decay time (s)	Ref.
SnO_2 nanobelt	–	20,000	~70[a]	RT	~220	~220	[32]
ZnO nanorod (NR)	~500[a]	200	4	RT	30–40	–	[14]
ZnO NW	100	100	34	RT	65	11	[16]
ZnO NW	~200	500	55	RT	75	50	[33]
Cd-doped ZnO NW		100		RT			[5]
	90		274		14	11	
	200		~40[a]		–	–	
ZnO:Ag NW	250	100	~50	RT	22	11	Current work

[a] Denotes a value approximated from a graphical plot or SEM images.

measured in air at RT at different values of dark current (0.1, 1.0, 2.5, 4.0, 6.0 and 8.0 nA). According to our experimental results presented in Fig. 8(b), it can be observed that UV response is dependent on applied bias voltage, and is decreasing as the applied voltages is increasing. The same tendency was also observed for ZnO nanotetrapods based photodetectors reported in a previous work [17]. Thus, at dark current of 0.1 nA, it can be observed an increase in the current value of about two orders in magnitude ($I_{UVON}/I_{UVOFF} \sim 52$) of a single ZnO:Ag NW under exposure to UV light. By increasing the dark current value to about 8 nA, the UV response was $I_{UVON}/I_{UVOFF} \sim 1.48$. A clear evidence on difference of the photocurrent rise time (τ_r) and decay time (τ_d) constants in dependence on the applied bias voltage also can be observed in Fig. 8(a). The fabricated nanosensors demonstrated fast response for all values of dark current and a good reproductibility, which are the most important parameters for a photodetector [17]. At 0.1 nA and 1.0 nA values of the dark current, it can be observed that photocurrent does not recover completely to the initial baseline (see Fig. 8(a)). A bi-exponential fitting was used to determine the slow and fast components of the time constants, using equations reported in a previous work [17]. The obtained results for fast (τ_{r1}) and slow (τ_{r2}) rise times and fast (τ_{d1}) and slow (τ_{d2}) decay times as a function of the dark current are presented in Fig. 8(d). As can be observed from Fig. 8(a and d) the constants τ_{r1}, τ_{d1} and τ_{d2} are decreased as the applied bias voltage, while constant τ_{r2} value was increased. The time constants τ_{r1}, τ_{r2}, τ_{d1} and τ_{d1} are 0.46, 0.63, 0.5 and 4.4 s, respectively, for dark currents of 0.1 nA; and 0.24, 1.64, 0.195 and 0.28 s, respectively, for dark current of 8.0 nA (Samples of ZnO:Ag nanowires with 1.0 μM $AgNO_3$ in the electrolyte). For samples fabricated from ZnO:Ag nanowires with 0.5 and 2.0 μM $AgNO_3$ in the electrolyte, it was slower, almost similar to previously reported values, as indicated in Table 2.

Thus, it can be concluded that photodesorption of oxygen molecules from the surface (τ_{r2}) of ZnO:Ag NW becomes slower due to an increase in applied bias voltage [31]. For a better demonstration of nanosensors fast response, short UV pulses with 0.25 s and 0.35 s durations were applied for three dark current values of 0.1 nA, 2.5 nA and 8.0 nA (see Fig. 8(b)). It is obvious that for a higher dark current value a sensitive and faster UV response was detected, while at lower dark current values the sensitivity is much higher. Fig. 8(e and f) shows the example of bi-exponential fitting of the photoresponse decay curve at dark current of 0.1 nA and photoresponse rise curve at dark current of 8.0 nA. In Table 1 the most relevant data on hydrogen gas sensor based on a single undoped and a single doped Q1D nanostructure are presented, in order to compare nanosensor performances obtained in current work with others reported in the literature. Gas response dependence on the diameter of Q1D nanostructures was demonstrated in a previous work [5]. However, as it can be observed from Table 1 by doping ZnO rods-wires with diameter 200–300 nm with silver ions, it was possible to shorten the hydrogen gas response time in comparison with that of the undoped SnO_2 nanobelt too, ZnO NW with lower diameter (D = 100 nm) or ZnO NW with a comparable diameter. Also ZnO:Ag nanorods-nanowires demonstrate faster response and recovery times in comparison with undoped nanostructures of ZnO and SnO_2. The hydrogen gas response in the case of ZnO:Ag was slightly higher in comparison with ZnO:Cd NW at the same diameter of the nanostructures (50% versus 40%), demonstrating possibility of use doped nanostructures with higher diameter for nanofabrication of faster and more reliable hydrogen gas sensor structures. In Table 2 experimental data on UV photo-detectors based on a single Q1D nanostructures reported previously and compared to the current results are presented. Table 2 demonstrates that our nanosensors based on a single ZnO:Ag nanorods–nanowires have very fast component of recovery time and even faster rise times in comparison with some of the best reports in literature, demonstrating good potential for fabrication of robust and fast UV photodetectors with low power consumption. By varying dark currents it is possible to obtain new UV photodetectors with high response (~52, in case of 0.1 nA) and with relatively slow recovery (~5 s) or to obtain a faster device structure with rise time ~0.97 s and decay time <0.98 s (Fig. 8(d)) but with

Table 2
Comparison of the UV photodetectors performances based on a single Q1D structure.

Material, morphology and diameter	Diameter (nm)	λ (nm)	Power of UV illumination (mW/cm^2)	UV on-off ratio	Response/rise time (s)	Recovery/decay time (s)	Rapid decay time, τ_{d1} (s)	Ref.
ZnO rod	~500[a]	370	–	1.03[a]	>300[a]	>300[a]	–	[34]
ZnO funct. SnO_2 NW	250	365	–	1.5	>180	>180	–	[35]
ZnO NW	50	370	–	~1.1[a]	120	180	–	[6]
ZnO NW	–	365	–	1.5×10^3	–	–	0.8	[36]
ZnO MW	1000–3000	370	0.1	~1.1[a]	>180[a]	>180[a]	–	[37]
ZnO MW	6000	325	24	9×10^5	6.28	–	0.85	[38]
ZnO:Ag rod-wire	250	365	15–20					Current work
I_{UVOFF} = 0.1 nA				~52	~1.09	~5	0.5	
I_{UVOFF} = 2.5 nA				~3.5	~1.11	~0.87	0.27	

[a] Denotes a value approximated from a graphical plot or SEM images.

lower UV response values (~3.5) (Fig. 8(c)) at dark current value of 2.5 nA.

4. Discussion and proposed sensing mechanism

Next, we discuss experimental results and present our proposed sensing mechanisms to explain data on UV response of the ZnO:Ag NW with control of Debye length $L \sim \lambda_D$ by acceptor doping with silver ions. The Ag incorporation at the interstitial (Ag_i) sites and the oxygen sites (Ag_O) are not efficient due to the high formation energies, while incorporation at the Zn sites (Ag_{Zn}) is the most energetically favorable [4,10]. It is known that silver ions act as acceptors in ZnO by substitution of the Zn^{2+} [39,40]. As a result, the net donor density (N_D) was decreased [40]. UV sensing mechanism and energy band bending of the undoped and single ZnO:Ag NW nanosensor are illustrated in Fig. 9. Since NWs possess a high surface-to-volume ratio, the surface of NW become highly active due to adsorbed oxygen species (O_2^-, O^{2-}, O^-) and is more influenced by the near-surface and surface defects [33,41], that can act as charge carriers traps as well as adsorption sites [25]. It is known that surface reactivity is dependent on the surface defects and doping of the zinc oxide NW [5,16,42]. Since Ag ions can be easily oxidized [43] it can act as a catalyst for oxygen ionization at the surface of ZnO NW [44], that leads to more adsorbed oxygen species on the NW surface. At room temperature the predominant species are oxygen molecules represented by the red double spheres in Fig. 9(a and b), which capture electrons from the NW and create an electron-depleted layer with low conductivity at the surface, which is shown by blue transparent region in Fig. 9, $O_{2(g)} + e^- \rightarrow O_{2(ad)}^-$ [45–47].

The thickness of the electron-depleted layers will be noted as L_{ZnO}, $L_{Ag\text{-}ZnO}$ for undoped and ZnO:Ag NW, respectively. The conduction channel was represented by the yellow region, and diameter was noted by d_{ZnO} for the ZnO NW and $d_{Ag\text{-}ZnO}$ for the ZnO:Ag NW (Fig. 9). The height of the interfacial potential in the dark/air was noted as $V_{S(1)}$. In a previous study, the ZnO:Ag NWs were found to be more oxygen deficient in comparison with the undoped sample, but with a higher crystallinity [9]. Thus, for ZnO:Ag NW, there are more hole trap surface states presented (Fig. 9(b)) and bulk defects to surface defects ratio is decreased [25,42], that leads to more narrowed conduction channel. As was reported in previous works [5,16,48], the thickness of the electron-depleted layer may depend on the Debye length $L \sim \lambda_D$ and on the interfacial potential $L \sim V_S^{1/2}$. The Debye length and interfacial potential are dependent on the N_D through the following relations [5,16]:

$$\lambda_D = \left(\frac{\varepsilon kT}{2\pi q^2 N_D}\right) \quad (1)$$

$$V_S = \frac{2\pi Q_s^2}{\varepsilon N_D} \quad (2)$$

where ε is the dielectric constant, k is the Boltzmann constant, T is the absolute temperature, q is the unit electron charge, and Q_s is the surface charge density.

Due to the formation of Ag acceptors, the N_D is decreased [40] and due to diminished bulk defects to surface defects ratio, the surface charge density (Q_s) was increased, leading to an increase of the λ_D (Eq. (1)) and V_S (Eq. (2)). As a result, the thickness of the electron-depleted layer $L_{Ag\text{-}ZnO}$ was increased ($L_{ZnO} < L_{Ag\text{-}ZnO}$, Eq. (1)), that leads to a narrower conduction channel for ZnO:Ag NW ($d_{ZnO} > d_{Ag\text{-}ZnO}$) (Fig. 9(b)). However, the electron-depleted layer thickness needs to be controlled accurately in the case of thinner NW, to avoid flat-band condition [5], thus L value needs to be smaller than half of NW diameter. Assuming that $qV_{S(1)}$ was ~1.45 eV and $N_{D(ZnO)} \sim 10^{18}\,cm^{-3}$ [40,49] for the undoped ZnO NW, the thickness of the electron-depleted layer at room temperature (300 K) may be estimated to be $L_{ZnO} \sim 35$ nm [49]. As well as, for ZnO:Ag NW $L_{Ag\text{-}ZnO} \sim 115$ nm, for $qV_{S(1)}$ was 1.55 eV and $N_{D(Ag\text{-}ZnO)} \sim 10^{17}\,cm^{-3}$ [40,49]. Thus, a thicker microwire doped with Ag can act as an efficient sensor structure too.

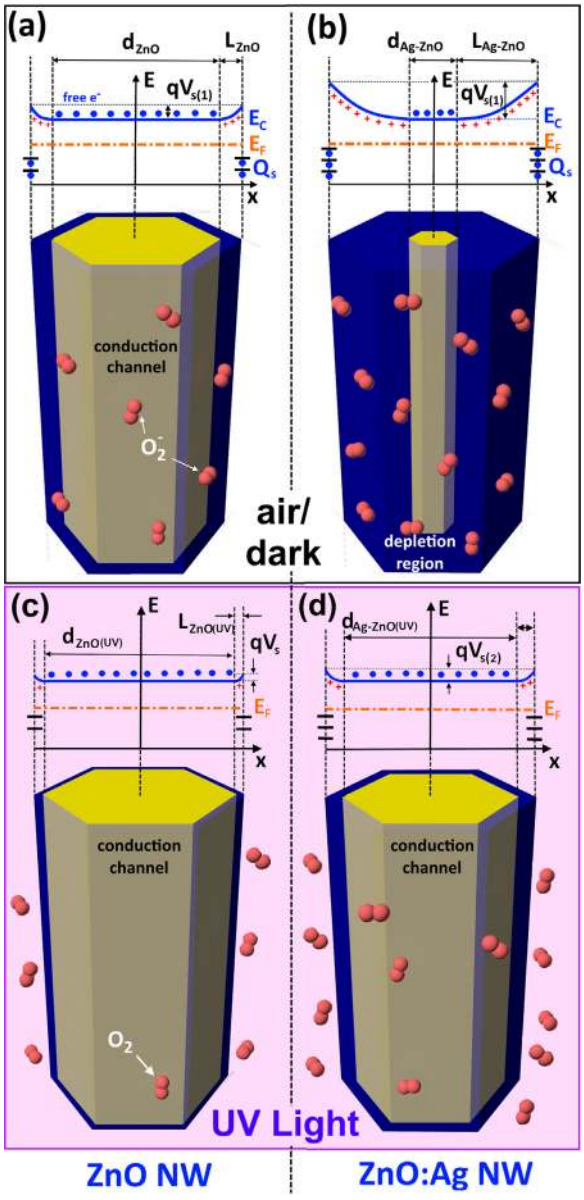

Fig. 9. Illustration of the UV sensing mechanism at room temperature of a single ZnO and ZnO:Ag NW based on ionosorption model and energy band diagram. (a) At exposure to ambient air, on the ZnO NW surface will be adsorbed oxygen molecule, represented by red double spheres, which by trapping of free electrons from the conduction band (CB) will lead to formation of the electron-depleted region (blue transparent zone) with width L_{ZnO} at the surface of the NW. The conduction channel was presented as yellow region. (b) In the case of ZnO:Ag NW, the width of electron-depleted region may be wider ($L_{Ag\text{-}ZnO}$) due to lower donor density and catalytic effect of Ag. At illumination with UV light (λ = 365 nm) the photo-desorption of oxygen molecules by generation of electron–hole pairs will take place and will lead to decrease of electron-depleted region and increase in conductivity of conduction channel (c and d). (For interpretation of the references to color in this figure legend, the reader is referred to the web version of the article.)

The UV detection mechanism was proposed extensively previously for pure ZnO and below we will try to explain our experimental data on UV response of the ZnO:Ag NW device (Fig. 8(a and b)). Under UV illumination (λ = 365 nm) of ZnO:Ag NW device (Fig. 9(a and b)), the electron–hole ($e^- + h^+$) pairs

(Fig. 9(c and d)) are generated in ZnO:Ag NW ($E = h\nu \rightarrow e^- + h^+$) [16], and are separated by the built-in electric field in the electron-depleted layer [16,47,50]. The photo-generated holes migrate to the surface of the NW to decrease the width of the electron-depleted layers $L_{ZnO(UV)}$ and $L_{Ag\text{-}ZnO(UV)}$ and to discharge adsorbed oxygen ions by the surface electron-hole recombination (Fig. 9(c and d), $h^+ + O_{2(ad)}{}^- \rightarrow O_{2(g)}$) [16,45–47].

As a result, unpaired electrons left in the conduction channel significantly contribute to an increase in the photocurrent of the NW (Fig. 8(a and b), UV on state) [16,45,46]. Kong et al. [42] and Liu et al. [25] reported that decrease of bulk to surface defects ratio can enhance the electron–hole separation efficiency, leading to photocurrent enhancement. However, if the UV light is turned off, the un-paired electrons recombine with holes generated at the re-adsorption and ionization of the oxygen species on the NW surface and nanosensor is returning to the initial value of the dark current (Fig. 8(a and b), UV off state) [31,45]. As was previously defined, the UV response of the un-doped and ZnO:Ag NW can be shown as $S_{UV} = I_{UVON}/I_{UVOFF}$. Due to narrower conduction channel of the ZnO:Ag NW, $d_{ZnO} > d_{O\text{-}Ag\text{-}ZnO}$ (Fig. 9(a and b)), the value of the I_{UVOFF} for ZnO:Ag NW is lower than that of pure ZnO NW which leads to a higher value of the response S_{UV} (Fig. 9(a)). Proposed mechanism for H_2 gas sensing of a single ZnO:Ag NW is presented in Fig. S2.

5. Conclusions

We demonstrated a novel type of multifunctional nanosensors based on a single ZnO:Ag nanowire electrodeposited on F-doped tin oxide (FTO) substrates, subsequent dispersion and its direct integration on the chip. Post-deposition thermal treatment at 250 °C in air was applied to activate dopant and to control the crystalline structure of NWs. Crystalline ZnO:Ag nanowires were studied by SEM, EDX, TEM, HRTEM, SIMS, X-ray photoelectron spectroscopy and micro-Raman spectroscopy. Integration of a single nanowire on the chip was performed by employing metal deposition function by using metal maskless nanodeposition in the dual beam focused electron/ion beam instrument. We found that ZnO:Ag NW nanosensors possess a much faster response/recovery times (~0.98 s/~0.87 s, respectively) and higher response to UV radiation and hydrogen gas at room temperature (~50%) and it can serve as nanomaterials for reliable, robust, ultrasensitive and ultra-rapid UV detectors and gas sensors with low power consumption. An increase in the current value of about two orders ($I_{UVON}/I_{UVOFF} \sim 52$) under illumination with UV light was observed at dark current of 0.1 nA. The mechanisms for such improved responses to single ZnO:Ag nanorod/nanowire are discussed based on ionosorption model and energy band diagrams. Developed nanosensors based on a single ZnO:Ag nanorods–nanowires have very fast component of recovery times and even faster rise times in comparison with some of the best reports in literature, demonstrating good potential for fabrication of robust and fast nanodevices with low power consumption. The developed nanomaterial could be of important scientific interest for further studies as promising candidates for fabricating multifunctional nano- and micro-sensors on *p*-type ZnO, light-emitting diodes, solar cells and photodetectors.

Acknowledgements

Dr. Lupan gratefully acknowledges the Alexander von Humboldt Foundation for the fellowship for experienced researchers at the University of Kiel, Germany. Christoph Ochmann and Stefan Rehders are acknowledged for their technical support. BRC acknowledges Grant NSF-DMR-1207065 and the Cluster of Excellence RESOLV (EXC 1069) at RUB funded by the Deutsche Forschungsgemeinschaft. This work was partially financially supported by the STCU under the Grant No. 5989.

Appendix A. Supplementary data

Supplementary data associated with this article can be found, in the online version, at http://dx.doi.org/10.1016/j.snb.2015.10.002.

References

[1] C.O. Chey, X. Liu, H. Alnoor, O. Nur, M. Willander, Fast piezoresistive sensor and UV photodetector based on Mn-doped ZnO nanorods, Phys. Status Solidi RRL 9 (2015) 87–91.
[2] L. Chow, O. Lupan, G. Chai, FIB fabrication of ZnO nanotetrapod and cross-sensor, Phys. Status Solidi B 247 (2010) 1628–1632.
[3] L. Chow, O. Lupan, G. Chai, H. Khallaf, L. Ono, B. Roldan Cuenya, I. Tiginyanu, V. Ursaki, V. Sontea, A. Schulte, Synthesis and characterization of Cu-doped ZnO one-dimensional structures for miniaturized sensor applications with faster response, Sens. Actuators A 189 (2013) 399–408.
[4] Y. Li, X. Zhao, W. Fan, Structural, electronic, and optical properties of Ag-doped ZnO nanowires: first principles study, J. Phys. Chem. C 115 (2011) 3552–3557.
[5] O. Lupan, L. Chow, T. Pauporté, L. Ono, B. Roldan Cuenya, G. Chai, Highly sensitive and selective hydrogen single-nanowire nanosensor, Sens. Actuators B 173 (2012) 772–780.
[6] O. Lupan, G. Chai, L. Chow, G. Emelchenko, H. Heinrich, V. Ursaki, A. Gruzintsev, I. Tiginyanu, A. Redkin, Ultraviolet photoconductive sensor based on single ZnO nanowire, Phys. Status Solidi A 207 (2010) 1735–1740.
[7] O. Lupan, V. Guérin, I. Tiginyanu, V. Ursaki, L. Chow, H. Heinrich, T. Pauporté, Well-aligned arrays of vertically oriented ZnO nanowires electrodeposited on ITO-coated glass and their integration in dye sensitized solar cells, J. Photochem. Photobiol. A 211 (2010) 65–73.
[8] M. Thomas, J. Cui, Electrochemical route to p-type doping of ZnO nanowires, J. Phys. Chem. Lett. 1 (2010) 1090–1094.
[9] O. Lupan, L. Chow, L.K. Ono, B. Roldan Cuenya, G. Chai, H. Khallaf, S. Park, A. Schulte, Synthesis and characterization of Ag- or Sb-doped ZnO nanorods by a facile hydrothermal route, J. Phys. Chem. C 114 (2010) 12401–12408.
[10] T. Pauporté, O. Lupan, J. Zhang, T. Tugsuz, I. Ciofini, F. Labat, B. Viana, Low temperature preparation of Ag-doped ZnO nanowire arrays, DFT study and application to light emitting diode, ACS Appl. Mater. Interfaces 7 (2015) 11871–11880.
[11] A. Mendoza-Galvan, C. Trejo-Cruz, J. Lee, D. Bhattacharyya, J. Metson, P. Evans, U. Pal, Effect of metal-ion doping on the optical properties of nanocrystalline ZnO thin films, J. Appl. Phys. 99 (2006) 014306.
[12] O. Lupan, T. Pauporté, T. Le Bahers, I. Ciofini, B. Viana, High aspect ratio ternary $Zn_{1-x}Cd_xO$ nanowires by electrodeposition for light-emitting diode applications, J. Phys. Chem. C 115 (2011) 14548–14558.
[13] H.S. Kang, B.D. Ahn, J.H. Kim, G.H. Kim, S.H. Lim, H.W. Chang, S.Y. Lee, Structural, electrical, and optical properties of p-type ZnO thin films with Ag dopant, Appl. Phys. Lett. 88 (2006) 202108.
[14] O. Lupan, G. Chai, L. Chow, Novel hydrogen gas sensor based on single ZnO nanorod, Microelectron. Eng. 85 (2008) 2220–2225.
[15] O. Lupan, V. Cretu, M. Deng, D. Gedamu, I. Paulowicz, S. Kaps, Y.K. Mishra, O. Polonskyi, C. Zamponi, L. Kienle, Versatile growth of freestanding orthorhombic α-molybdenum trioxide nano- and microstructures by rapid thermal processing for gas nanosensors, J. Phys. Chem. C 118 (2014) 15068–15078.
[16] O. Lupan, V. Ursaki, G. Chai, L. Chow, G. Emelchenko, I. Tiginyanu, A. Gruzintsev, A. Redkin, Selective hydrogen gas nanosensor using individual ZnO nanowire with fast response at room temperature, Sens. Actuators B 144 (2010) 56–66.
[17] D. Gedamu, I. Paulowicz, S. Kaps, O. Lupan, S. Wille, G. Haidarschin, Y.K. Mishra, R. Adelung, Rapid fabrication technique for interpenetrated ZnO nanotetrapod networks for fast UV sensors, Adv. Mater. 26 (2014) 1541–1550.
[18] G.S. Aluri, A. Motayed, A.V. Davydov, V.P. Oleshko, K.A. Bertness, N.A. Sanford, R.V. Mulpuri, Methanol, ethanol and hydrogen sensing using metal oxide and metal (TiO_2–Pt) composite nanoclusters on GaN nanowires: a new route towards tailoring the selectivity of nanowire/nanocluster chemical sensors, Nanotechnology 23 (2012) 175501.
[19] J. Jiménez, H. Liu, E. Fachini, X-ray photoelectron spectroscopy of silver nanoparticles in phosphate glass, Mater. Lett. 64 (2010) 2046–2048.
[20] N. Watanabe, H. Yamashita, H. Miyadera, S. Tominaga, Removal of unpleasant odor gases using an Ag–Mn catalyst, Appl. Catal. B: Environ. 8 (1996) 405–415.
[21] Y. Wu, C. Jiang, C. Wan, R. Holze, Composite materials of silver and natural graphite as anode with low sensibility to humidity, J. Power Sources 112 (2002) 255–260.
[22] S. Zanna, C. Saulou, M. Mercier-Bonin, B. Despax, P. Raynaud, A. Seyeux, P. Marcus, Ageing of plasma-mediated coatings with embedded silver

nanoparticles on stainless steel: an XPS and ToF-SIMS investigation, Appl. Surf. Sci. 256 (2010) 6499–6505.
[23] C. Arguello, D. Rousseau, S.P.d.S. Porto, First-order Raman effect in wurtzite-type crystals, Phys. Rev. 181 (1969) 1351.
[24] W. Li, C. Kong, H. Ruan, G. Qin, G. Huang, T. Yang, W. Liang, Y. Zhao, X. Meng, P. Yu, Electrical properties and Raman scattering investigation of Ag doped ZnO thin films, Solid State Commun. 152 (2012) 147–150.
[25] D. Liu, Y. Lv, M. Zhang, Y. Liu, Y. Zhu, R. Zong, Y. Zhu, Defect-related photoluminescence and photocatalytic properties of porous ZnO nanosheets, J. Mater. Chem. A 2 (2014) 15377–15388.
[26] X. Wang, C. Song, K. Geng, F. Zeng, F. Pan, Luminescence and Raman scattering properties of Ag-doped ZnO films, J. Phys. D: Appl. Phys. 39 (2006) 4992.
[27] H. Khallaf, G. Chai, O. Lupan, H. Heinrich, S. Park, A. Schulte, L. Chow, Investigation of chemical bath deposition of ZnO thin films using six different complexing agents, J. Phys. D: Appl. Phys. 42 (2009) 135304.
[28] S. Shishiyanu, O. Lupan, E. Monaico, V. Ursaki, T. Shishiyanu, I. Tiginyanu, Photoluminescence of chemical bath deposited ZnO:Al films treated by rapid thermal annealing, Thin Solid Films 488 (2005) 15–19.
[29] O. Lupan, T. Pauporté, I. Tiginyanu, V. Ursaki, V. Sontea, L. Ono, B. Roldan Cuenya, L. Chow, Comparative study of hydrothermal treatment and thermal annealing effects on the properties of electrodeposited micro-columnar ZnO thin films, Thin Solid Films 519 (2011) 7738–7749.
[30] M. Enachi, O. Lupan, T. Braniste, A. Sarua, L. Chow, Y.K. Mishra, D. Gedamu, R. Adelung, I. Tiginyanu, Integration of individual TiO_2 nanotube on the chip: nanodevice for hydrogen sensing, Phys. Status Solidi RRL 9 (2015) 171–174.
[31] C. Soci, A. Zhang, B. Xiang, S.A. Dayeh, D. Aplin, J. Park, X. Bao, Y.-H. Lo, D. Wang, ZnO nanowire UV photodetectors with high internal gain, Nano Lett. 7 (2007) 1003–1009.
[32] L. Fields, J. Zheng, Y. Cheng, P. Xiong, Room-temperature low-power hydrogen sensor based on a single tin dioxide nanobelt, Appl. Phys. Lett. 88 (2006) 3102.
[33] S.N. Das, J.P. Kar, J.-H. Choi, T.I. Lee, K.-J. Moon, J.-M. Myoung, Fabrication and characterization of ZnO single nanowire-based hydrogen sensor, J. Phys. Chem. C 114 (2010) 1689–1693.
[34] O. Lupan, L. Chow, G. Chai, L. Chernyak, O. Lopatiuk-Tirpak, H. Heinrich, Focused-ion-beam fabrication of ZnO nanorod-based UV photodetector using the in-situ lift-out technique, Phys. Status Solidi A 205 (2008) 2673–2678.
[35] Q. Kuang, C.-S. Lao, Z. Li, Y.-Z. Liu, Z.-X. Xie, L.-S. Zheng, Z.L. Wang, Enhancing the photon- and gas-sensing properties of a single SnO_2 nanowire based nanodevice by nanoparticle surface functionalization, J. Phys. Chem. C 112 (2008) 11539–11544.
[36] Y. Hu, J. Zhou, P.H. Yeh, Z. Li, T.Y. Wei, Z.L. Wang, Supersensitive, fast-response nanowire sensors by using Schottky contacts, Adv. Mater. 22 (2010) 3327–3332.
[37] G. Chai, L. Chow, O. Lupan, E. Rusu, G. Stratan, H. Heinrich, V. Ursaki, I. Tiginyanu, Fabrication and characterization of an individual ZnO microwire-based UV photodetector, Solid State Sci. 13 (2011) 1205–1210.
[38] J. Dai, C. Xu, X. Xu, J. Guo, J. Li, G. Zhu, Y. Lin, Single ZnO microrod ultraviolet photodetector with high photocurrent gain, ACS Appl. Mater. Interfaces 5 (2013) 9344–9348.
[39] S.-T. Kuo, W.-H. Tuan, J. Shieh, S.-F. Wang, Effect of Ag on the microstructure and electrical properties of ZnO, J. Eur. Ceram. Soc. 27 (2007) 4521–4527.
[40] J. Fan, R. Freer, The roles played by Ag and Al dopants in controlling the electrical properties of ZnO varistors, J. Appl. Phys. 77 (1995) 4795–4800.
[41] O. Lupan, L. Chow, G. Chai, A single ZnO tetrapod-based sensor, Sens. Actuators B 141 (2009) 511–517.
[42] M. Kong, Y. Li, X. Chen, T. Tian, P. Fang, F. Zheng, X. Zhao, Tuning the relative concentration ratio of bulk defects to surface defects in TiO_2 nanocrystals leads to high photocatalytic efficiency, J. Am. Chem. Soc. 133 (2011) 16414–16417.
[43] Y. Zheng, L. Zheng, Y. Zhan, X. Lin, Q. Zheng, K. Wei, Ag/ZnO heterostructure nanocrystals: synthesis, characterization, and photocatalysis, Inorg. Chem. 46 (2007) 6980–6986.
[44] I.-S. Hwang, J.-K. Choi, H.-S. Woo, S.-J. Kim, S.-Y. Jung, T.-Y. Seong, I.-D. Kim, J.-H. Lee, Facile control of C_2H_5OH sensing characteristics by decorating discrete Ag nanoclusters on SnO_2 nanowire networks, ACS Appl. Mater. Interfaces 3 (2011) 3140–3145.
[45] Y. Jin, J. Wang, B. Sun, J.C. Blakesley, N.C. Greenham, Solution-processed ultraviolet photodetectors based on colloidal ZnO nanoparticles, Nano Lett. 8 (2008) 1649–1653.
[46] H. Kind, H. Yan, B. Messer, M. Law, P. Yang, Nanowire ultraviolet photodetectors and optical switches, Adv. Mater. 14 (2002) 158–160.
[47] G. Chai, O. Lupan, L. Chow, H. Heinrich, Crossed zinc oxide nanorods for ultraviolet radiation detection, Sens. Actuators A 150 (2009) 184–187.
[48] G. Chai, O. Lupan, E. Rusu, G. Stratan, V. Ursaki, V. Şontea, H. Khallaf, L. Chow, Functionalized individual ZnO microwire for natural gas detection, Sens. Actuators A 176 (2012) 64–71.
[49] J. Goldberger, D.J. Sirbuly, M. Law, P. Yang, ZnO nanowire transistors, J. Phys. Chem. B 109 (2005) 9–14.
[50] G. Cheng, X. Wu, B. Liu, B. Li, X. Zhang, Z. Du, ZnO nanowire Schottky barrier ultraviolet photodetector with high sensitivity and fast recovery speed, Appl. Phys. Lett. 99 (2011) 203105.

Biographies

Oleg Lupan is a fellow for experienced researchers supported by Alexander von Humboldt Foundation at CAU, Germany. He received his M.S. in microelectronics and semiconductor devices from the Technical University of Moldova (TUM) in 1993. He received his Ph.D. in solid state electronics, microelectronics and nanoelectronics from the Institute of Applied Physics, Academy of Sciences of Moldova (ASM) in 2005. His post-doctorate research activities were carried out at the French CNRS, Paris, France and the University of Central Florida, USA. He received his doctor habilitate degree in 2011 from the Institute of Electronic Engineering and Nanotechnologies of ASM. He is an Associate Professor and researcher scientist in solid state electronics and nanoelectronics at TUM. His current research interests include sensors, optoelectronic devices, nanotechnologies and nanodevices.

Vasilii Cretu is a senior lecturer at the Technical University of Moldova (TUM) and is a PhD candidate in the group of Nanotechnologies for sensing nanodevices, Moldova. He received his M.Sc. in microelectronics and nanotechnologies from the Technical University of Moldova in 2008. Since 2010 he has been a PhD student in nanotechnologies and physics of nanosystems at TUM. He received 3rd place at the competition "Laureate in field of Technical Creativity" at TUM in 2013. His research interests include nanotechnologies of semiconducting oxides, chemical and electrochemical synthesis, sensors.

Vasile Postica is at present a candidate in the group of Nanotechnologies for sensing nanodevices, Moldova. He worked in the field of zinc oxide–copper oxide composite and its surface modification for his Engineering degree diploma (ranked as the best one at TUM in 2014 year) and continued for master thesis in Nanotechnologies at Technical University of Moldova. His current research interest is nanostructuring of semiconducting oxides, thin films, gas sensors and UV photodetectors' development.

Mahdi Ahmadi is a PhD student in the Physics Department at the University of Central Florida (UCF). He joined Prof. Roldan's group at UCF after finishing his M.Sc in Optics-Physics at the University of Tehran (Iran) and his B.Sc in Physics at the Sharif University of Technology (Iran). His current research interests are the physical and chemical properties of nanoparticles and their applications in nanocatalysis.

Beatriz Roldan Cuenya is a professor in the Department of Physics at the Ruhr-University Bochum (Germany). She was previously (2004–2013) a professor at the University of Central Florida (Orlando, USA). Beatriz did her postdoctoral research in the Department of Chemical Engineering at the University of California Santa Barbara (2001–2003). She obtained her PhD from the Department of Physics at the University of Duisburg-Essen (Germany) in 2001. She completed her M.S./B.S. in Physics with a minor in Materials Science from the University of Oviedo, Spain in 1998. Her research program explores novel physical and chemical properties of size- and shape-selected nanostructures, with emphasis on advancements in nanocatalysis (http://www.ep4.rub.de).

Lee Chow is a Professor at the Department of Physics University of Central Florida Orlando. He received his B.S. in physics in 1972 from the National Central University, Taiwan. He received Ph.D. in Physics from Clark University, Worcester, MA, USA in 1981. In 1980–1982 he was a postdoc in physics at the University of North Carolina, Chapel Hill, NC. He joined University of Central Florida in 1983 as an assistant Professor, and was promoted to associate professor in 1988 and to professor in 1998. Areas of expertise: Chemical bath deposition, nanofabrications of carbon nanotubes and metal oxides, diffusion in semiconductors, high T_c and diamond thin films.

Ion Tiginyanu received his Ph.D. degree in Semiconductor Physics from Lebedev Institute of Physics, Moscow, in 1982, and became full professor in 1993 at the Technical University of Moldova. Starting from 2001, he serves as the founding Director of the National Center for Materials Study and Testing. In 2013 he was elected prime vice-president of the Academy of Sciences of Moldova. Professor Tiginyanu's research interests are related to nanotechnologies, ultrathin membranes, 3D hybrid nanomaterials, photonic crystals, random lasing, cost-effective solar cells and new sensor technologies. He is member of AAAS, OSA, SPIE, MRS, IEEE and Electrochemical Society. More information is available at http://www.ncmst.utm.md.

Bruno Viana (1962, Paris, France) got a PhD degree in Materials Science at University P&M Curie, Paris in 1987. He was laureate as CNRS researcher in 1988. In 2003 he became Director of Research at the French Research council CNRS. In 2010–2013, he was at the head of the "Photonics Research Group". In 2014 he became responsible of the CNRS research network CMDO+ (http://cmdo.cnrs.fr/). Dr Bruno VIANA is currently a Senior Scientist in IRCP Chimie-Paristech Institute working on the preparation and the characterization of Optical Materials for photonics.

Thierry Pauporté is director of research at the Centre National de la Recherché Scientifique (CNRS) in France and he works at Chimie-Paristech. He is graduated in Chemistry from the École Normale Supérieure de Lyon. He received his Ph.D. in physical chemistry from Montpellier II University, France, in 1995. Dr. Th. Pauporté has made original and innovative contributions to the synthesis, characterization and understanding of fundamental chemical and physical properties of oxide films and nanostructures. He also works on hybrid perovskites. He is also interested in the functionalizing of the material surfaces and he works on the integration of films and structures in efficient devices. The applications studied include light emitting diodes, perovskite solar cells, dye-sensitized solar cells, nanosensors, photodetectors, photocatalysis, wettability, fouling, etc.

Rainer Adelung is full professor and Chairholder of Functional Nanomaterials group established in 2007 at the Institute for Materials Science, University of Kiel, Germany. He received Ph.D. (rer. net) in Physics in 2000 from Institute of Experimental and Applied Physics, University of Kiel and during 2001–2002 he was at Case Western Reserve University in Cleveland (USA) as Feodor Lynen (Alexander von Humboldt) Research Fellow. In 2006 he finished Habilitation at Institute for Materials Science in Kiel and then continued as Heisenberg Professor (DFG grant) with his own Functional Nanomaterials group till 2012.